Vacancies and deep levels in electron-irradiated 6*H* SiC epilayers studied by positron annihilation and deep level transient spectroscopy

A. Kawasuso,[a] F. Redmann, and R. Krause-Rehberg
Martin-Luther-Universität, FB Physik, D-06099 Halle, Germany

T. Frank, M. Weidner, and G. Pensl
Universität Erlangen-Nürnberg, Staudtstrasse 7, D-91058 Erlangen, Germany

P. Sperr
Universität der Bundeswehr München, D-85577 Neubiberg, Germany

H. Itoh
Japan Atomic Energy Research Institute, 1233, Watanuki, Takasaki, Gunma, 370-1292, Japan

(Received 12 March 2001; accepted for publication 16 July 2001)

The annealing behavior of defects in *n*-type 6*H* SiC epilayers irradiated with 2 MeV electrons have been studied using positron annihilation and deep level transient spectroscopy. Vacancy-type defects are annealed at 500–700 °C and 1200–1400 °C. From the analysis of Doppler broadening spectra (core electron momentum distribution), the latter annealing process is attributed to the disappearance of complexes related to silicon vacancies and not to nearest neighbor divacancies. Among the observed deep levels, the E_1/E_2 levels show similar annealing behavior to that of positron annihilation centers above 1000 °C. It is thus proposed that the E_1/E_2 levels originate from complexes containing silicon vacancies. © *2001 American Institute of Physics.*
[DOI: 10.1063/1.1402144]

I. INTRODUCTION

Photoluminescence (PL)[1,2] and deep level transient spectroscopy (DLTS)[3–11] studies on 6*H* SiC show that a number of deep centers are generated by particle bombardment. These deep centers have important roles in application since: (i) ion implantation is an indispensable step for the selective doping of SiC[12,13] and (ii) special radiation-induced defects can be used to control minority carrier lifetime.[14] One current interest in this subject is to identify the microscopic origin of radiation-induced deep centers.

The D_1 luminescence in 6*H* SiC is considered to originate from complexes associated with intrinsic defects.[1,2] This luminescence appears due to postirradiation annealing at approximately 1000 °C and survives even at 1700 °C. In addition to the D_1 luminescence, several PL bands are introduced by bombardment.[9,15,16] More than ten deep levels have been observed in *n*-type 6*H* SiC irradiated with fast particles. Among them the E_1/E_2 and Z_1/Z_2 levels exhibit remarkable high thermal stability. In early studies, it is reported that the Z_1/Z_2 levels are thermally stable up to 1700 °C.[17] Recent studies show that the Z_1/Z_2 levels induced by He irradiation are reduced below 1400 °C.[9,18] Gong *et al.* reported that the E_1/E_2 levels are predominant after electron irradiation and subsequent annealing at 1100 °C.[8] Frank *et al.* observed that the E_1/E_2 levels and the D_1 luminescence show a correlation in their annealing behavior.[9] It is also reported that the E_1/E_2 levels show the negative-*U* character.[6,7] The atomic structure of the E_1/E_2 and Z_1/Z_2 levels have not yet been clarified adequately as well as that of the D_1 luminescence.

Recently, high quality epitaxial layers were successfully produced.[19] This provides us with an opportunity to study point defects in SiC with less influence from grown-in defects. Microscopic identification of radiation-induced defects in 6*H* SiC epilayers has been extensively carried out with the optically detected magnetic resonance (ODMR) technique. Sörman *et al.*[15] specified a PL band originating from isolated silicon vacancies with a theoretical support by Zywietz *et al.*[20,21] Son *et al.*[22] found a characteristic ODMR spectrum after electron irradiation, which is attributed to nearest neighbor divacancies or complexes associated with silicon vacancies. Due to its superior selectivity to vacancy-type defects, positron annihilation spectroscopy (PAS) is also used for the study of SiC.[23–34] In this work, we performed PAS and DLTS measurements for *n*-type 6*H* SiC epilayers irradiated with 2 MeV electrons. We report the annealing behavior of vacancy-type defects and their correlation with the E_1/E_2 levels induced by electron irradiation.

II. EXPERIMENT

The samples used in this study were cut from a high-quality 6*H* SiC epilayer (5 μm thick) grown on a 3.5° off oriented SiC (0001) substrate, which was purchased from Cree Research Inc. The epitaxial layer exhibited *n*-type conductivity (doped with nitrogen) with a net donor concentration of 5×10^{15} cm^{-3} at room temperature. As a reference, a *p*-type epilayer with a net acceptor concentration of 5×10^{15} cm^{-3} (doped with aluminum) was used. The *n*-type epilayers were irradiated with 2 MeV electrons at doses of

[a]Author to whom correspondence should be addressed; permanent address: Japan Atomic Energy Research Institute, 1233, Watanuki, Takasaki, Gunma, 370-1292, Japan; electronic mail: kawasuso@physik.uni-halle.de

 © 2001 American Institute of Physics

Downloaded 01 Oct 2001 to 133.53.228.253. Redistribution subject to AIP license or copyright, see http://ojps.aip.org/japo/japcr.jsp

1×10^{15} and 3×10^{17} e^-/cm^2 for DLTS and PAS measurements, respectively, at 40 °C. Isochronal annealing was carried out in the temperature range from 100 to 1700 °C for 30 min in vacuum or dry argon ambient. Above 1500 °C, the samples were annealed in a SiC crucible to avoid the sublimation of Si atoms from the sample surfaces. After fabricating Schottky and ohmic contacts using Ni, DLTS measurements were performed in the temperature range from 100 to 600 K. Details of the DLTS experiments will be described elsewhere.[35]

Positron lifetime measurements were carried out with a pulsed positron beam at 17 keV.[36] The system time resolution was 260 ps at full width at half maximum. After subtracting one long-lived component (typically ~500 ps with intensities less than 3%), which comes from instruments, average positron lifetimes were determined by the PATFIT program.[37] The positron bulk lifetime was determined to be 140 ± 2 ps using the *p*-type epilayer.[38] This is in good agreement with the theoretical bulk lifetime of SiC.[39] The Doppler broadening of annihilation radiation (511 keV) was measured as a function of incident positron energy E from 0.1 to 39 keV using a Ge detector. Furthermore, the coincidence Doppler broadening measurements[40] were also performed to determine detailed momentum distribution of core electrons. The normalized peak and tail intensities (defined as S and W parameters) were determined from the obtained spectra. Here, energy windows were selected to be 511.0–511.8 keV for S parameters and 516.0–522.0 keV for W parameters. Vacancy-type defects are detected as increase in S parameter and decrease in W parameter relative to the value for defect free state denoted by S_B and W_B. Both *n*-type and *p*-type as-grown epilayers exhibited unique S and W parameters at $E>25$ keV ($S=0.4342\pm0.0004$ and $W=0.0034\pm0.0002$). Considering the result of positron lifetime measurements, these were characterized as S_B and W_B. All the S and W parameters obtained in this work were normalized to S_B and W_B, respectively.

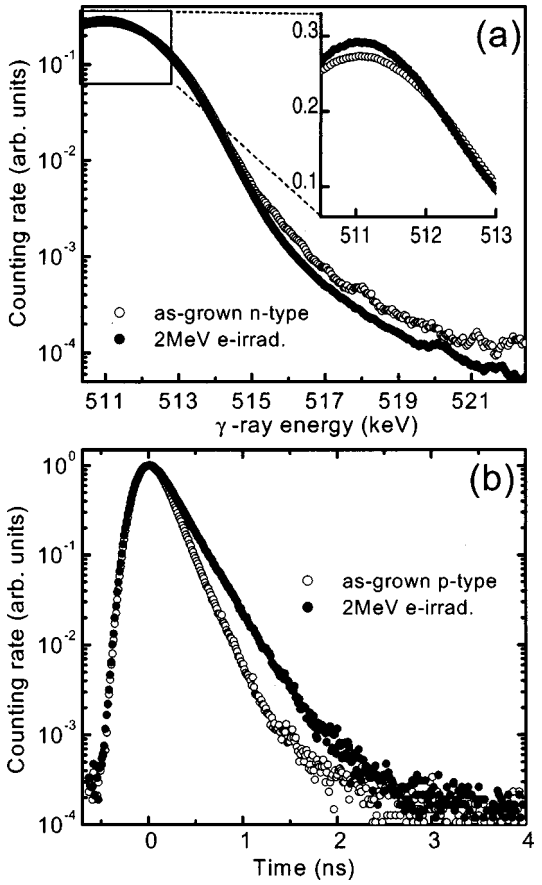

FIG. 1. (a) The Doppler broadening spectra for the as-grown sample (open circle) and the electron-irradiated sample at a dose of 3×10^{17} e^-/cm^2 (solid circle). The inset shows the magnification of the central region in linear scale. The incident positron energy is 20 keV. These spectra are normalized to their area intensities. (b) Positron lifetime spectra for the reference (as-grown *p*-type) sample (open circle) and the electron-irradiated sample at a dose of 3×10^{17} e^-/cm^2 (solid circles). The incident positron energy is 17 keV. These spectra are normalized at the peak intensities.

III. RESULTS AND DISCUSSION

A. Positron annihilation

Figure 1(a) shows the normalized Doppler broadening spectra for the as-grown sample and electron-irradiated sample at a dose of 3×10^{17} e^-/cm^2. It is found that the peak and tail intensities (i.e., S and W parameters) increase and decrease, respectively, after electron irradiation. Figure 1(b) shows the corresponding positron lifetime spectra for the reference (as-grown *p*-type epilayer) and the electron-irradiated sample. Positron lifetime increases after irradiation. The average positron lifetime for the electron-irradiated sample was determined to be 194 ps. This is sufficiently greater than the bulk lifetime (140 ± 2 ps) determined for the reference sample. The above positron annihilation spectra show that vacancy-type defects are introduced in the epilayer by electron irradiation.

Figure 2(a) shows the S parameter as a function of incident positron energy for the as-grown sample and electron-irradiated sample at a dose of 3×10^{17} e^-/cm^2. (The upper horizontal axis shows the mean positron implantation depth deduced from an empirical formula.[41]) The S parameter for the as-grown sample increases in the low energy region ($E<5$ keV). A similar feature has already been reported previously.[42–44] This is explained by the diffusion of positrons to the surface. That is, the annihilation from the surface state and/or the reemission from the surface. The S parameter is almost constant at $E>20$ keV suggesting that most positrons annihilate in the bulk region. The S parameter for the electron-irradiated sample is greater than that of the as-grown sample at $E>5$ keV and only weakly depends on the incident positron energy. We also evaluated the R parameters ($R=|(S-S_B)/(W-W_B)|$), which depend on the type of defect and not on the concentration.[45] Figure 2(b) shows the R parameter for the electron-irradiated sample as a function of incident positron energy. The R parameter is almost constant at $E>5$ keV. Thus, vacancies are homogeneously produced by electron irradiation. Although it is expected that a part of positrons penetrate into a deeper region beyond the interface between epilayer and substrate at $E>35$ keV, this effect seems to be small in both the as-grown and electron-irradiated sample as seen from Fig. 2.

Downloaded 01 Oct 2001 to 133.53.228.253. Redistribution subject to AIP license or copyright, see http://ojps.aip.org/japo/japcr.jsp

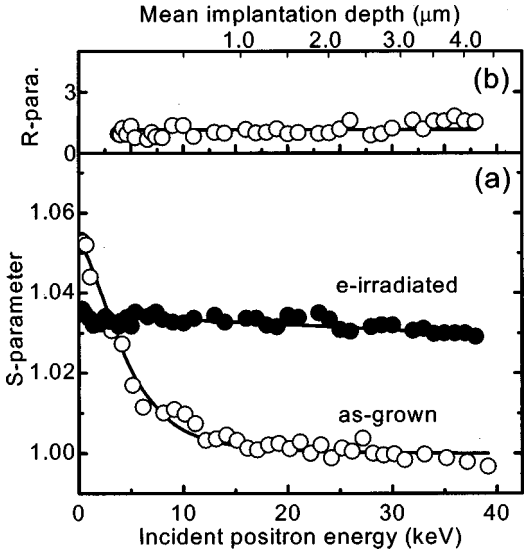

FIG. 2. (a) *S* parameter for the as-grown sample (open circle) and the electron-irradiated sample at a dose of 3×10^{17} e^-/cm^2 (solid circle) as a function of incident positron energy. (b) *R* parameters for the electron-irradiated sample as a function of incident positron energy. The upper horizontal axis shows the mean positron implantation depth deduced from an empirical formula.

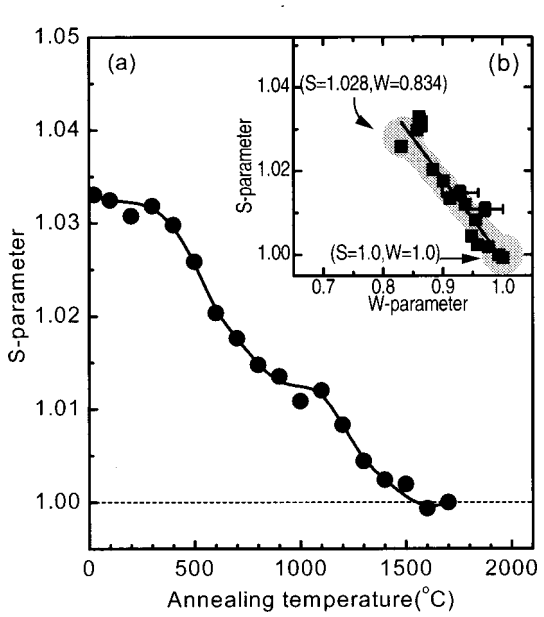

FIG. 3. (a) Annealing behavior of the *S* parameter for the electron-irradiated sample at a dose of 3×10^{17} e^-/cm^2 deduced by the VEPFIT analysis. The annealing duration is 30 min. (b) *S* vs *W* plot through annealing. The gray circles at ($S=1.0$, $W=1.0$) and ($S=1.028$, $W=0.834$) indicate the locations of (*S*, *W*) data for the as-grown state (fully annealed state) and silicon vacancies determined previously, respectively.

The above *S*–*E* relations are further analyzed in the one-dimensional diffusion model with a Makhovian type positron implantation profile and an empirically determined mean implantation depth.[40,46] The energy-dependent *S* parameter is generally treated as the stacking of layers. That is, in the present case, the *S* parameter for the as-grown and the electron-irradiated sample can be described with two terms related to the surface and one layer (epilayer):

$$S(E)=F_S(E)S_S+F_L(E)S_L, \tag{1}$$

where S_S and S_L are the *S* parameters for the surface and the layer, respectively, and $F_S(E)$ and $F_L(E)$ are the respective fractions of positron annihilation ($F_S(E)+F_L(E)=1$). In the analysis, S_S, S_L, and the positron diffusion length are given as initial parameters and their optimum values are determined by the least square fitting method using the VEPFIT program.[47] The solid lines shown with the *S* parameter in Fig. 2 are the results of the VEPFIT analysis. Here, epithermal positrons were not taken into account since the fitting results were not significantly altered by this term. The above one layer model reproduces the experimental *S*–*E* relations for both the as-grown and electron-irradiated samples very well. For the as-grown sample, S_L and the effective diffusion length in the layer were determined to be 1.000 ± 0.002 and 160.4 nm, respectively. Taking $\tau_B=140$ ps as bulk lifetime, the diffusion coefficient of positrons is estimated to be 1.8 cm^2/s. This value is comparable to the typical diffusion coefficient in semiconductors.[45] Thus, the as-grown sample contains few positron trapping and/or scattering sites. The *S* parameter and diffusion length in the damage layer of the electron-irradiated sample are evaluated to be 1.033 ± 0.002 and 6.3 nm, respectively. The reduced effective diffusion length indicates that most positrons annihilate in the damage layer.

Vacancy-type defects giving rise to the average positron lifetime and *S* parameter to be 194 ps and 1.033, respectively, are homogeneously created by electron irradiation. Theoretical study based on the linear muffin-tin orbital atomic sphere approximation by Brauer *et al.*[39] shows that positron lifetimes for a carbon vacancy, a silicon vacancy, and a nearest neighbor divacancy in 6*H* SiC are 153, 194, and 217 ps, respectively. Recent calculation employing the plane wave pseudopotential by Staab *et al.*[48] also shows similar positron lifetimes for a silicon vacancy and a divacancy. It is also shown that the effect of inequivalent lattice sites in hexagonal SiC on positron lifetimes is fairly small (within a few ps). From several experiments,[27,34] positron lifetimes for carbon vacancies and silicon vacancies are determined to be 160 and 189 ps, respectively, which are in good agreement with the theory. The average positron lifetime after electron irradiation (194 ps) coincides with the theoretical positron lifetime for silicon vacancies. The *S* parameter (1.033) is also in good agreement with the specific *S* parameter (1.028–1.031) for isolated silicon vacancies in 3C SiC.[23–25,49]

Figure 3(a) shows the *S* parameter for the electron-irradiated sample at a dose of 3×10^{17} e^-/cm^2 obtained from the VEPFIT analysis as a function of annealing temperature. It is found that the *S* parameter first decreases at 500–700 °C and finally recovers to the as-grown state above 1200 °C. Figure 3(b) shows the *S* versus *W* plot through annealing. Here, the gray circle at ($S=1.0$, $W=1.0$) corresponds to the as-grown state (also, fully annealed state). As a comparison, the (*S*, *W*) data for isolated silicon vacancies determined previously[49] is also displayed by another gray circle at ($S=1.028$, $W=0.834$). The *S*–*W* correlation is more or less on

Downloaded 01 Oct 2001 to 133.53.228.253. Redistribution subject to AIP license or copyright, see http://ojps.aip.org/japo/japcr.jsp

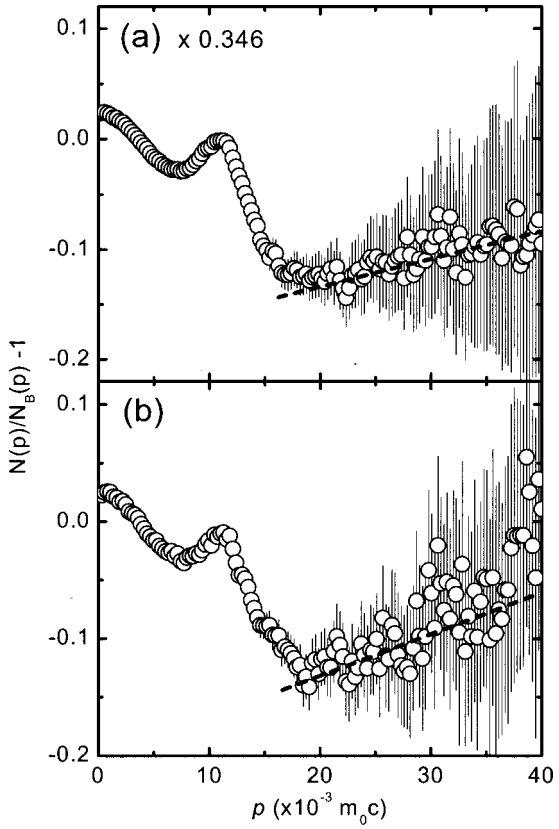

FIG. 4. The Doppler broadening spectra determined by the coincidence method after dividing by the spectrum for the as-grown sample and subtracting unity, i.e., $N(p)/N_B(p)-1$ for the electron-irradiated sample at a dose of 3×10^{17} e^-/cm^2 (a) at the as-irradiated state and (b) after annealing at 1000°C for 30 min. The vertical axis of (a) is scaled by multiplying with 0.343. Dashed lines in the figure are a guide for the eye to see the increases in intensities at $p>20\times10^{-3}m_0c$.

a straight line between these two positions. This linear correlation between S and W parameters indicates that silicon vacancy related defects are the major positron trapping centers and their chemical surroundings do not change significantly through annealing although the S parameter itself shows the two-step recovery in Fig. 3(a).

To see the above circumstances in more detail, the coincidence Doppler broadening measurements were performed. Figure 4 shows the so-called ratio spectra for the as-irradiated and 1000 °C annealed states as a function of electron–positron momentum p calculated from $\Delta E=cp/2$, where ΔE and c are the Doppler shift and light speed, respectively ($\Delta E=1$ keV corresponds to $p=3.91\times10^{-3}m_0c$). That is, to enhance the defect contribution, the original spectra are divided by the spectrum of the as-grown sample and subtracted by unity, i.e., $N(p)/N_{SiC}(p)-1$. For direct comparison of the line shapes between as-irradiated and 1000 °C annealed states, the vertical axis is further scaled so that two spectra overlap at $p=0$. The intensities of the ratio spectra are enhanced and suppressed at $p<3\times10^{-3}m_0c$ and $p>15\times10^{-3}m_0c$, respectively, due to annihilation of positrons at vacancy-type defects.[45] The line shapes of the two ratio spectra mostly overlap. This fact supports the above discussion based on the S–W correlation that the dominant defect species are likely to be conserved even after annealing at 1000 °C. The valence electron contribution vanishes up to $p=20\times10^{-3}m_0c$ and hence core electron contribution is important at $p>20\times10^{-3}m_0c$.[48] Despite the large statistical error, the ratio spectra show a tendency to increase at $p>20\times10^{-3}m_0c$. Staab *et al.*[48] show that the Doppler spectrum of SiC in the high momentum region exhibits different features for carbon vacancies, silicon vacancies, and divacancies. The intensity of the ratio spectrum for carbon vacancies should decrease with increasing momentum at $p>20\times10^{-3}m_0c$. This feature is attributed to the enhancement of annihilation probability with silicon core electrons (mainly $2sp$) giving rise to a relatively narrow Doppler shift. In contrast, the intensity of the ratio spectrum for silicon vacancies should increase. This is because of the enhancement of annihilation probability with carbon core electrons ($1s$) giving rise to a relatively large Doppler shift. For divacancies, these opposite tendencies for carbon and silicon vacancies are mutually canceled and hence the ratio curve does not depend strongly on momentum. The apparent increases in the ratio spectra at $p>20\times10^{-3}m_0c$ shown in Fig. 4 exhibit the character of carbon core electrons, i.e., positron annihilation centers should accompany silicon vacancies at least.

The reason why silicon vacancies are the major positron trapping centers is also discussed from the radiation damage theory. Considering the threshold energy ($E_d\sim30$ eV) for the atomic displacement in SiC,[50] the average primary knock-on atom energy (E_{PKA}) due to collisions with 2 MeV electrons is estimated to be approximately 70 eV. Then the damage function ($\nu=E_{PKA}/2E_d$) is approximately unity. Accordingly, single vacancies and interstitials on both Si and C sublattices may be the main products of irradiation. The concentration of divacancies is expected to be small. Carbon vacancies are reported to disappear upon annealing below 200 °C.[51,52] The effect of carbon vacancies is not distinctly seen in the above results. This is probably explained as the small differences of S and W parameters for carbon vacancies from those for bulk because of the weak localization of positrons at carbon vacancies.[28,48,49] Alternatively, this might be due to much lower positron trapping efficiency of carbon vacancies.

The above results and discussion lead us to the conclusion that silicon vacancy related defects act as the major positron trapping centers after electron irradiation. The annealing stage at 500–700 °C in Fig. 3(a) is consistent with that of isolated silicon vacancies.[15,49,53] The residual component after the annealing at 700 °C should be related to complexes including silicon vacancies, which have higher thermal stability than isolated silicon vacancies. Previous studies for highly nitrogen doped bulk 6H SiC also show that vacancy-type defects finally disappear at around 1400 °C after electron irradiation. From the positron lifetime, this annealing step is proposed to be due to the disappearance of complexes related to silicon vacancies.[32] The similar ratio spectra of the coincidence Doppler measurements before and after annealing at 1000 °C in Fig. 4 imply that the adjacent elements of silicon vacant sites in the complexes are not much different from carbon atoms.

Downloaded 01 Oct 2001 to 133.53.228.253. Redistribution subject to AIP license or copyright, see http://ojps.aip.org/japo/japcr.jsp

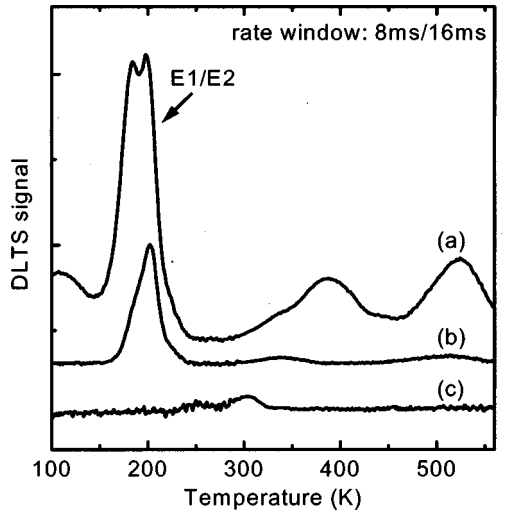

FIG. 5. DLTS spectra for the sample after electron irradiation at a dose of 1×10^{15} e^-/cm^2 and subsequent annealing at (a) 300 °C (i.e., after the first scan), (b) 1000 °C, and (c) 1400 °C. The rate window is 8 ms/16 ms.

B. Correlation between vacancies and deep levels

To see the correlation between vacancies and deep levels, DLTS measurements were performed. Figure 5 shows the DLTS spectra for the electron-irradiated sample at a dose of 1×10^{15} e^-/cm^2 after annealing at 300 °C (i.e., after the first scan), 1000 °C and 1400 °C. Four major peaks appear at approximately 200, 330, 390, and 530 K after annealing at 300 °C. The energy levels of the peaks at 200 and 530 K are determined to be $E_C-0.37\pm0.01$ eV and $E_C-1.15\pm0.06$ eV, respectively, with temperature independent capture cross sections ($\sim1\times10^{-15}$ cm^2). It was difficult to separate two overlapping peaks at 330 and 390 K and to determine individual energy levels. Instead, their average energy level is determined to be $E_C-0.68\pm0.02$ eV. Considering the past studies,[11,18,35] the above four peaks are assigned to the E_1/E_2, Z_1/Z_2, *L*9, and *R* centers, respectively.

The concentration of the E_1/E_2 levels is determined to be approximately 2×10^{14} cm^{-3}. The concentrations of the other levels are approximately one order of magnitude lower than that of the E_1/E_2 levels. From the change of its line shapes during annealing, it is found that one more level overlaps the E_1 level as reported by Gong *et al.*[8] After 1200 °C annealing, the concentration of all the levels except the E_1/E_2 levels are almost below the detection limit. This is in good agreement with the results obtained by Gong *et al.*[8] From its high thermal stability, it is inferred that the E_1/E_2 levels originate from complexes rather than simple vacancies and interstitials.

Among the observed levels, the E_1/E_2 levels show comparable annealing behavior with PAS detected vacancies in the high temperature annealing process. For the comparison between PAS and DLTS data, the positron trapping rate, which is proportional to the defect concentration, is calculated from

$$\kappa=\tau_B^{-1}(S-S_B)/(S_V-S), \tag{2}$$

where S_V is the specific *S* parameter for vacancies.[45] Here, we assumed $S_V=1.028$ for silicon vacancies.[49] Figure 6

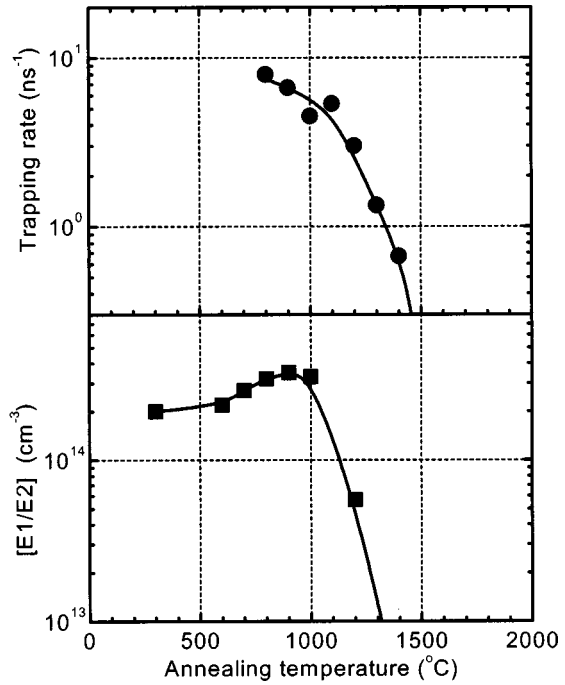

FIG. 6. Annealing behavior of (a) the positron trapping rate calculated from Eq. (2) with $S_D=1.028$ for the electron-irradiated sample at a dose of 3×10^{17} e^-/cm^2 and (b) the concentration of the E_1/E_2 levels observed in the electron-irradiated sample at a dose of 1×10^{15} e^-/cm^2.

shows the annealing behavior of the concentration of the E_1/E_2 levels. It is found that the annealing curves of the positron trapping rate and the concentration of the E_1/E_2 levels are in good agreement above 900 °C. Only the E_1/E_2 levels show a comparable annealing behavior with PAS detected vacancies. Although hole traps were not observed in this study, Gong *et al.*[54] reported that all the hole traps in *p*-type 6*H* SiC epilayers irradiated by 1.7 MeV electrons are drastically annealed below 600 °C. Thus, the E_1/E_2 levels are most likely to be correlated with PAS detected vacancies. As shown above, the PAS detected defects are related to silicon vacancies. It is therefore concluded that the E_1/E_2 levels originate from complexes associated with silicon vacancies. The divacancy model for the E_1/E_2 levels[8] proposed recently is not confirmed here although silicon vacancies should be one of the constituents in the defects responsible for the E_1/E_2 levels. Since the electron doses for the PAS and DLTS samples are different, the above comparison is qualitative. Nevertheless, any ambiguities arising from the history of crystal itself, e.g., grown-in defects, impurities are largely reduced because all samples are cut from the same epilayer.

IV. CONCLUSIONS

In conclusion, we have studied the annealing process of vacancy-type defects and deep centers in *n*-type 6*H* SiC epilayers irradiated with 2 MeV electrons. It is found that silicon vacancy related defects are the major positron trapping centers. They are annealed in two stages at 500–700 and 1200–1400 °C. Isolated silicon vacancies and complexes including silicon vacancies, respectively, are considered to be responsible for these two annealing processes. From the cor-

Downloaded 01 Oct 2001 to 133.53.228.253. Redistribution subject to AIP license or copyright, see http://ojps.aip.org/japo/japcr.jsp

relation between positron annihilation and DLTS data, it is proposed that the E_1/E_2 levels originate from silicon vacancy related complexes.

ACKNOWLEDGMENTS

One of the authors (A.K.) thanks the Alexander von Humboldt Stiftung for their support in conducting this research project. They are also grateful to J. Gebauer of Lawrence Berkeley National Laboratory for a fruitful discussion on the coincidence Doppler measurements.

[1] W. J. Choyke, Inst. Phys. Conf. Ser. **31**, 58 (1977).
[2] L. Patrick and W. J. Choyke, Phys. Rev. B **5**, 3253 (1972).
[3] V. S. Ballandovich and G. N. Violina, Cryst. Lattice Defects Amorphous Mater. **13**, 189 (1987).
[4] J. P. Doyle, M. O. Aboelfotoh, M. K. Linnarsson, B. G. Svensson, A. Schöner, N. Nordell, D. Harris, J. L. Lindström, E. Janzén, and C. Hemmingsson, Mater. Res. Soc. Symp. Proc. **423**, 519 (1996).
[5] C. Hemmingsson, N. T. Son, O. Kordina, E. Janzén, and J. L. Lindström, J. Appl. Phys. **84**, 704 (1998).
[6] C. Hemmingsson, N. T. Son, and E. Janzén, Appl. Phys. Lett. **74**, 839 (1999).
[7] C. Hemmingsson, N. T. Son, O. Kordina, J. L. Lindström, and E. Janzén, Semicond. Sci. Technol. **14**, 251 (1999).
[8] M. Gong, S. Fung, C. D. Beling, and Z. You, J. Appl. Phys. **85**, 7604 (1999).
[9] T. Frank, G. Pensl, S. Bai, R. P. Devaty, and W. J. Choyke, Mater. Sci. Forum **338–342**, 753 (2000).
[10] A. A. Lebedev, A. I. Veinger, D. V. Davydov, V. V. Kozlovski, N. S. Savkina, and A. M. Strel'chuk, J. Appl. Phys. **88**, 6265 (2000).
[11] V. S. Ballandovich, Sov. Phys. Semicond. **33**, 1188 (1999).
[12] T. Kimoto, N. Inoue, and H. Matsunami, Phys. Status Solidi A **162**, 263 (1997).
[13] T. Troffer, M. Schadt, T. Frank, H. Itoh, G. Pensl, J. Heindl, H. P. Strunk, and M. Maier, Phys. Status Solidi A **162**, 277 (1997).
[14] N. T. Son, E. Sörman, W. M. Chen, O. Kordina, B. Monemar, and E. Janzén, Appl. Phys. Lett. **65**, 2687 (1994).
[15] E. Sörman, N. T. Son, W. M. Chen, O. Kordina, C. Hallin, and E. Janzén, Phys. Rev. B **61**, 2613 (2000).
[16] N. T. Son, E. Sörman, M. Singh, W. M. Chen, C. Hallin, O. Kordina, and E. Janzén, Diamond Relat. Mater. **6**, 1378 (1997).
[17] G. Pensl and W. J. Choyke, Physica B **185**, 264 (1993).
[18] T. Dalibor, G. Pensl, H. Matsunami, T. Kimoto, W. J. Choyke, A. Schöner, and N. Nordell, Phys. Status Solidi A **162**, 199 (1997).
[19] T. Kimoto, A. Itoh, and H. Matsunami, Phys. Status Solidi B **202**, 247 (1997).
[20] A. Zywietz, J. Furthmüller, and F. Bechstedt, Phys. Rev. B **61**, 13655 (2000).
[21] A. Zywietz, J. Furthmüller, and F. Bechstedt, Phys. Rev. B **59**, 15166 (1999).
[22] N. T. Son, O. N. Hai, M. Wagner, W. M. Chen, A. Ellison, C. Hallin, B. Monemar, and E. Janzén, Semicond. Sci. Technol. **14**, 1141 (1999).
[23] H. Itoh, M. Yoshikawa, L. Wei, S. Tanigawa, I. Nashiyama, S. Misawa, H. Okumura, and S. Yoshida, Mater. Res. Soc. Symp. Proc. **262**, 331 (1992).
[24] H. Itoh, M. Yoshikawa, I. Nashiyama, L. Wei, S. Tanigawa, S. Misawa, H. Okumura, and S. Yoshida, Mater. Sci. Forum **117–118**, 501 (1993).
[25] H. Itoh, M. Yoshikawa, I. Nashiyama, L. Wei, S. Tanigawa, S. Misawa, H. Okumura, and S. Yoshida, Hyperfine Interact. **79**, 725 (1993).
[26] A. I. Girka, V. A. Kuleshin, A. D. Mokrushin, E. N. Mokhov, S. V. Svirida, and A. V. Shishkin, Sov. Phys. Semicond. **23**, 1337 (1989).
[27] A. A. Rempel and H.-E. Schaefer, Appl. Phys. A: Mater. Sci. Process. **61**, 51 (1995).
[28] S. Dannefaer, D. Craigen, and D. Kerr, Phys. Rev. B **51**, 1928 (1995).
[29] A. Polity, S. Huth, and M. Lausmann, Phys. Rev. B **59**, 10603 (1999).
[30] C. C. Ling, A. H. Deng, S. Fung, and C. D. Beling, Appl. Phys. A: Mater. Sci. Process. **70**, 33 (2000).
[31] A. Kawasuso, H. Ito, D. Cha, and S. Okada, Mater. Sci. Forum **264–268**, 611 (1998).
[32] A. Kawasuso, H. Ito, S. Okada, and H. Okumura, J. Appl. Phys. **80**, 5639 (1996).
[33] A. Kawasuso, H. Ito, T. Ohshima, K. Abe, and S. Okada, J. Appl. Phys. **82**, 3232 (1997).
[34] A. Kawasuso, H. Ito, N. Morishita, M. Yoshikawa, T. Ohshima, I. Naishyama, S. Okada, H. Okumura, and S. Yoshida, Appl. Phys. A: Mater. Sci. Process. **67**, 209 (1998).
[35] T. Frank, M. Weidner, A. Kawasuso, H. Itoh, and G. Pensl (unpublished).
[36] P. Sperr and G. Kögel, Mater. Sci. Forum **255–257**, 109 (1997).
[37] P. Kirkegaard, N. Pederson, and M. Eldrup, PATFIT-88, Riso-M-2704 (1989).
[38] The as-grown *n*-type epilayer was unsuitable to determine exact bulk lifetime because of the reemission effect. The reemission effect vanishes for *p*-type and irradiated *n*-type epilayers.
[39] G. Brauer, W. Anward, E.-M. Nicht, J. Kuriplach, M. Sŏb, N. Wagner, P. G. Poleman, M. J. Puska, and T. Korhonen, Phys. Rev. B **54**, 2512 (1996).
[40] J. Gebauer, R. Krause-Rehberg, S. Eichler, and F. Böner, Appl. Surf. Sci. **149**, 110 (1999).
[41] J. Gebauer, S. Eichler, R. Krause-Rehberg, and H. P. Zeindl, Appl. Surf. Sci. **116**, 247 (1997).
[42] A. Uedono, S. Tanigawa, T. Ohshima, H. Itoh, U. Aoki, M. Yoshikawa, and I. Nashiyama, J. Appl. Phys. **86**, 5392 (1999).
[43] A. Uedono *et al.*, J. Appl. Phys. **86**, 5392 (1999).
[44] T. Ohshima, A. Uedono, K. Abe, H. Itoh, U. Aoki, M. Yoshikawa, S. Tanigawa, and I. Nashiyama, Appl. Phys. A: Mater. Sci. Process. **67**, 407 (1998).
[45] R. Krause-Rehberg and H. S. Leipner, *Positron Annihilation in Semiconductors*, Springer Series in Solid-State Sciences, Vol. 127 (Springer, Berlin, 1998).
[46] K. G. Lynn, D. O. Welch, J. Throwe, and B. Nielsen, Int. Mater. Rev. **36**, 1 (1991).
[47] A. van Veen, H. Schut, M. Clement, J. M. M. de Nijs, A. Kruseman, and M. R. Ijpma, Appl. Surf. Sci. **85**, 216 (1995).
[48] T. Staab, L. M. Torpo, M. J. Puska, and R. M. Nieminen, Mater. Sci. Forum **353–356**, 533 (2001).
[49] A. Kawasuso, F. Redmann, R. Krause-Rehberg, M. Yoshikawa, K. Kojima, and H. Itoh, Phys. Status Solidi B **223**, R8 (2001).
[50] A. L. Barry, B. Lehmann, D. Fritsch, and D. Bräung, IEEE Trans. Nucl. Sci. **30**, 1111 (1991).
[51] H. Itoh, A. Kawasuso, T. Ohshima, M. Toshikawa, I. Nashiyama, S. Tanigawa, S. Misawa, H. Okumura, and S. Yoshida, Phys. Status Solidi A **162**, 173 (1997).
[52] D. Cha, H. Itoh, N. Morishita, A. Kawasuso, T. Ohshima, Y. Watanabe, J. Ko, K. Lee, and I. Nashiyama, Mater. Sci. Forum **264–268**, 615 (1998).
[53] H. Itoh, N. Hayakawa, I. Nashiyama, and E. Sakuma, J. Appl. Phys. **66**, 4529 (1989).
[54] M. Gong, S. Fung, C. D. Beling, and Z. You, J. Appl. Phys. **85**, 7120 (1999).

Downloaded 01 Oct 2001 to 133.53.228.253. Redistribution subject to AIP license or copyright, see http://ojps.aip.org/japo/japcr.jsp